*Atmósfera (1994)*, **7**, *pp. 143-158*

# Large–scale modes of variations in the global sea surface temperatures and Northern Hemisphere tropospheric circulation

ERNEST C. KUNG and JONQ–GONG CHERN

*University of Missouri–Columbia, Columbia, Missouri 65211, USA*

JOEL SUSSKIND

*Laboratory for Atmospheres, Goddard Space Flight Center/NASA, Greenbelt, Maryland 20771, USA*

(Manuscript received Sept. 22, 1993; accepted in final form Nov. 3, 1993)

RESUMEN

Se examinan los modos de variación de las temperaturas de la superficie del océano (SST's) y la circulación troposférica, con componentes principales mayores, empleando campos medios mensuales de las temperaturas superficiales globales del mar y las isohipsas (Z) a 700, 500 y 300 mb del Hemisferio Norte. El periodo de datos cubierto es de 1955 hasta 1992. Se encuentra que la heterogeneidad de los datos de temperatura debida a la disponibilidad de las observaciones de satélite y la diferencia en los esquemas de análisis puede resultar en un sesgo sistemático grande en el juego de datos.

Sin embargo, el sesgo puede ser corregido efectivamente mediante la eliminación de una componente principal apropiada.

Se presentan las tres primeras componentes de los campos de SST y de geopotencial Z durante el periodo de 38 años. Asimismo, se observa el modo de variaciones de El Niño–Oscilación Suriana (ENSO) en ambas componentes, 1a. y 2a. de las temperaturas oceánicas superficiales (SSTs). Las variaciones interanuales de las componentes principales de los campos mensuales de SST y Z se utilizan para indagar la asociación de las componentes de las SST y de las Z.

Más aún, los patrones de correlación cruzada de las componentes principales de las SSTs con referencia a la circulación troposférica son estudiados con los campos de isohipsas de 500 y 300 mb. Se muestra que la respuesta troposférica a las anomalías de SST son congruentes a los niveles de 500 y 300 mb y la predictibilidad de plazo estacional de la circulación troposférica se reconoce con los campos de anomalías de la temperatura oceánica superficial.

ABSTRACT

Large–scale modes of variations in sea surface temperatures (SSTs) and the tropospheric circulation are examined with major principal components utilizing monthly mean fields of the global SSTs and Northern Hemisphere geopotential height (Z) at 700, 500 and 300 mb levels. The data period covered is from 1955 to 1992. It is found that the heterogeneity of SST data due to availability of satellite observations and difference of analysis schemes may result in a large systematic bias in the dataset. However, the bias may be effectively corrected through elimination of an appropriate principal component.

The first three components of monthly SST and Z fields during the 38–year period are presented. The El Niño-Southern Oscillation (ENSO) mode of variations is observed in both 1st and 2nd components of SSTs. The inter–annual viariations of principal components of monthly SST and Z fields are utilized to probe the association of SST components and Z components.

Further, cross-correlation patterns of principal components of SSTs in reference to the tropospheric circulation are studied with 500 and 300 mb fields. It is hown that the tropospheric response to SST anomalies are consistent at 500 and 300 mb levels, and the seasonal-range predictability of the tropospheric circulation is recognized with SST anomaly fields.

## 1. Introduction

It is well recognized that the ocean surface provides a major boundary forcing to the general circulation of the atmosphere through the process of ocean–atmosphere heat transfer. A systematic investigation of the sea surface temperature (SST) anomalies in reference to the tropospheric circulation is thus a desired step toward better understanding of climatic fluctuations. This study is one such attempt by means of principal component analysis to identify prevailing modes of variations in SSTs and the tropospheric circulation.

The utility of the principal components, which are also referred to as empirical orthogonal functions or eigenvectors, in analyzing the large-scale variations of the circulation field has been demonstrated by Kutzbach (1967, 1970), Kidson (1975a, b), Weare *et al.* (1976), Weare (1977), Barnett (1978), Heddinghaus and Kung (1980), Trenberth and Paolino (1981), Kawamura (1984, 1986), Park and Kung (1988) and others. One goal of such an analysis is to reduce a large number of variables into a manageable set of components, while retaining the maximum variance of the original variables, enabling us to concisely describe patterns of interrelationship among observed variables. In the analysis of highly correlated meteorological fields, a limited number of principal components may effectively represent the fundamental modes of variations which are highly loaded on these components. It is important to note that the empirical orthogonal functions have no predetermined forms, and only depend on the interrelationship within the dataset of analysis. Thus, they are particularly suitable to investigate anomalous fields of the general circulation for which no known analytical form exists because of complex boundary conditions and various scales of nonlinear interactions.

In this study, pattern vectors and time coefficients are obtained for major principal components of monthly mean fields of the global SSTs and the Northern Hemisphere geopotential height Z(m) at 700, 500 and 300 mb. Variances of intra–annual seasonal variations are eliminated by defining the anomaly fields of monthly means in reference to the long–term means of individual months for the entire data period from 1955 to 1992. The characteristics of the first three components of SST fields are identified and discussed. The quality of SST data changes significantly during the data period because of the availability of satellite observations in the later years. The heterogeneity of data in time series is examined, and the elimination of bias is considered. The intra–annual seasonal variations of SSTs are also presented with principal components of long–term means of twelve individual months. The association of SST components and Z components is studied on the basis of inter–annual variations of these components. Cross–correlations of SST components with the observed Z fields are further studied to examine the seasonal–range predictability of the tropospheric circulation in reference to SST anomalies.

## 2. Data and scheme of analysis

Datasets utilized in this study include monthly global SST analyses for the period of 1955-92, and daily Northern Hemisphere Z analyses at 700, 500 and 300 mb for the same period. Monthly SST analyses were obtained from two different sources: the Comprehensive Ocean–Atmosphere Data Set (COADS) (Slutz *et al.*, 1985) for the period of 1955-79 and the NMC SST real–time analyses (Reynolds, 1988) for the period 1970-92. Both analyses are on $2^{\circ} \times 2^{\circ}$latitude–longitude

grids, but the grid points of these two analyses are staggered. The consistency of both analyses was verified for the overlapping period of 1970-79, and the COADS analysis of 1958-69 was interpolated on the grid points of the Reynolds analysis to make a complete time series of 1955-92. Missing data points in early COADS analysis were interpolated in space from the surrounding grid points. The SST data were used for the oceanic areas between 40°S to 60 °N. The monthly Z fields were computed from the daily National Meteorological Center (NMC) Northern Hemisphere octogonal grid analyses at 1500 GMT from 1955-57, and at 1200 GMT for the rest of the period.

The general mathematical procedures for computation of orthogonal pattern vectors and their coefficients are as provided in Kutzbach (1967). The grid values of monthly mean fields are standardized to zero mean and unit variance so that each grid point can have normalized significance in describing the spatial variation. As stated in the introduction, the anomaly fields are obtained with respect to the multi–annual means of respective monthly mean fields for the study of inter–annual variations. This allows for the elimination of the seasonal cycle. On the other hand, the intra–annual seasonal cycle is presented by subjecting the multi–annual means of 12 individual months to principal component analysis. The variable matrix, which has normalized departures from time means, is used to compute the corresponding correlation matrix, whose elements are the correlation between grid points. The eigenvectors of such a correlation matrix represent a set of normalized departure fields. The eigenvectors are not rotated in order to retain the maximum variance in the first few components (Walsh and Richman, 1981). The characteristic pattern vector is described as the eigenvector multiplied by the standard deviaton of its corresponding principal component. Thus, characteristic patterns represent the simple correlations between respective components and meteorological fields.

Most of the available principal component analyses of large–scale meteorological fields indicate that the first three components are sufficient to describe the large–scale variations (e.g., Kutzbach, 1970; Weare *et al.*, 1976; Weare, 1977; Park and Kung, 1988). As discussed by Overland and Preisendorfer (1982), it is important to determine if the principal components obtained in the analysis are statistically significant, so that the geophysical interpretation of results will be meaningful. As shown in pattern vector of major components (Figs. 2, 4, 5, 6 and 7), large–scale characteristic patterns are described mostly by large correlation coefficients of | 0.4 | to | 0.8 |, which are significant at the 98 to 99.9% confidence level for the time period of datasets. The higher components also show some significance in limited areas, but the level of significance in large areas drops sharply. In this paper, the discussion is limited to the first three components.

## 3. Principal components of SST fields

The inter–annual variations of coefficients of 1st principal components of January and July SSTs for the period of 1955-92, as shown in Figure 1, indicate a large gap at 1970. This phenomenon is also observed in all other months. If the SST data for the period of 1970-92 are subjected to principal component analysis, the 1st and 2nd components of the new time series match almost exactly with the 2nd and 3rd components of the original 1955-92 time series. The discontinuity of the 1955-92 data at 1970 in the 1st principal component is important as the 1st component contributes 18% of the total variance, and is larger than any other component's contribution. This gap indicates a major systematic difference of SST data before and after (including) 1970, most likely reflecting both the inclusion of satellite data and a different scheme of analysis in NMC data from that in earlier COADS records.

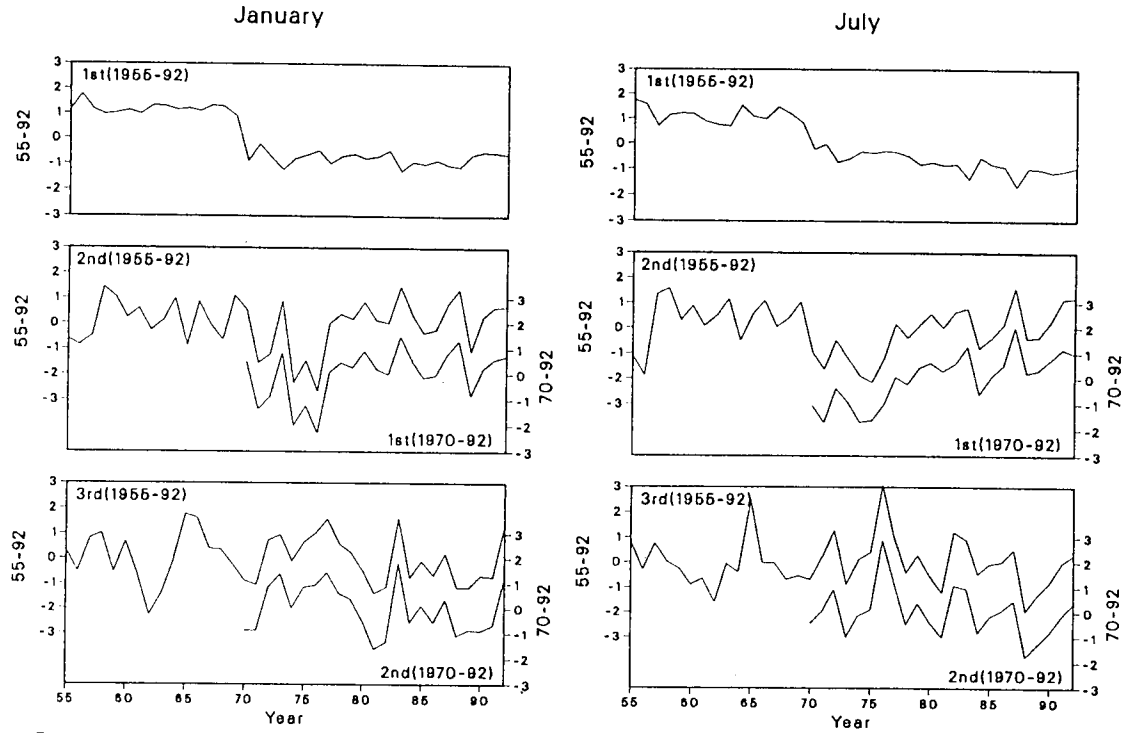


Fig. 1. Inter-annual variations of coefficients of the principal components 1, 2 and 3 for the original January and July SST datasets during the entire data period of 1955-92 and the partial data period of 1970-92.

In this study, the original 1st component in the 1955-92 dataset is disregarded, and the 2nd, 3rd and 4th components are treated as the true 1st, 2nd and 3rd components of the 1955-92 period. The principal components to be discussed hereafter refer to the true components after elimination of the original 1st component as a systematic bias. This is justified by the near exact match of the 1st and 2nd components of the 1970-92 dataset with the 2nd and 3rd components of the 1955-92 datasets. Since we are only interested in the first few major components, small-scale variations that are associated with the original 1st component, other than the gap at 1970, do not enter into the picture and can be ignored.

Figure 2 shows the pattern vectors for the first three components of January and July SSTs, and their corresponding coefficients are shown in Figure 3. The percentage variances of the first five components out of the total 35 components, listed in Table 1, indicate a comparable contribution of the first few components with previously available principal component analyses (see citations in Section 2). The pattern vectors of the 1st components, as shown in Figure 2, represent the largest-scale spatial variation in the Pacific and Atlantic. The variation in the northwest-southeast direction is conspicuous in the Pacific with a maximum positive area in the tropical region. The 2nd component shows a well defined positive area in the eastern tropical Pacific, which is similar to the 1st component previously obtained in the regional analyses of the Pacific SSTs (e.g., Weare, 1977; Weare *et al.*, 1976). Much of the other areas in the Pacific and Atlantic are negative, contrasting the large positive areas of the 1st component. The 3rd component shows variations in the Pacific and Atlantic in the norwest-southeast direction. The pattern vectors beyond the 3rd component show a localized, fragmental pattern, and are not included in our discussion of large-scale SST variations.

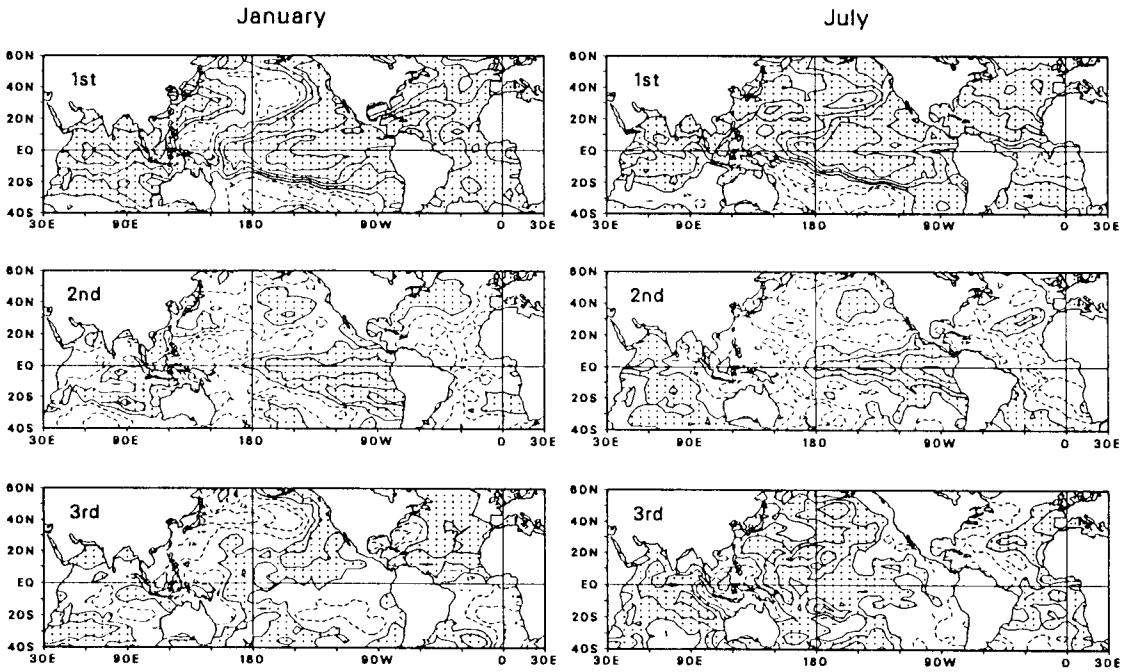


Fig. 2. Characteristic patterns (pattern vectors) for the first three principal components of January and July SSTs during the period of 1955-92. Positive areas are shaded. The contour interval is 0.2.

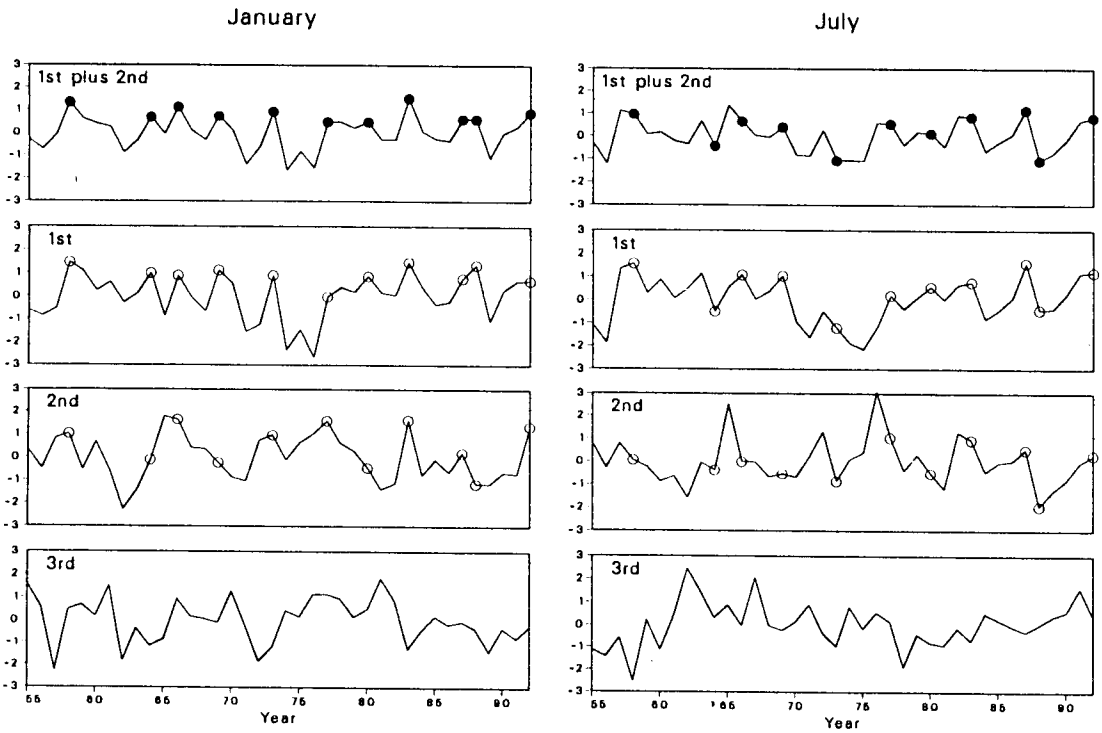


Fig. 3. Inter-annual variations of coefficients of the first three principal components of January and July SSTs during the period of 1955-92. Dots denote years of major winter ENSO episodes.

Table 1. Percentage variance of the first five principal components during the period of 1955-92

| Component | SST | | Z(700mb) | | Z(500mb) | | Z(300mb) | |
|---|---|---|---|---|---|---|---|---|
| | Jan. | July | Jan. | July | Jan. | July | Jan. | July |
| 1 | 17.1 | 12.2 | 17.5 | 17.1 | 17.7 | 20.0 | 20.0 | 22.1 |
| 2 | 7.4 | 8.6 | 15.5 | 9.9 | 13.0 | 8.7 | 13.2 | 12.0 |
| 3 | 5.6 | 5.5 | 9.3 | 8.9 | 10.3 | 8.5 | 8.9 | 7.0 |
| 4 | 5.0 | 5.2 | 8.7 | 7.3 | 9.0 | 6.8 | 7.6 | 5.8 |
| 5 | 4.4 | 4.9 | 6.4 | 5.9 | 6.3 | 5.6 | 6.7 | 5.0 |
| Total | 39.5 | 36.4 | 57.4 | 49.1 | 56.3 | 49.6 | 56.4 | 51.9 |

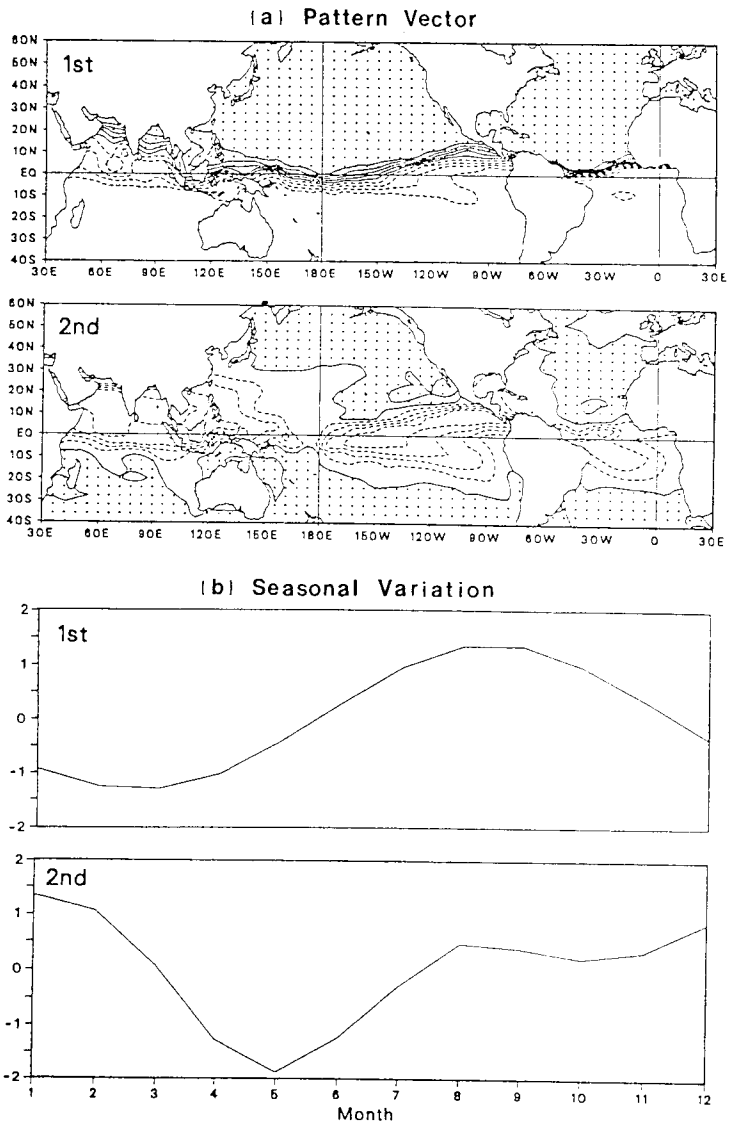


Fig. 4. (a) Characteristic patterns for the first two components of long-term (1955-92) mean monthly SSTs, and (b) corresponding coefficients of principal components. Positive areas are shaded. The contour interval is 0.2.

It is apparent that the pattern vectors of the 2nd component represent the El Niño–Southern Oscillation (ENSO) type of SST anomalies. Since the 1st component also has a general postive area in the central and eastern tropical Pacific, it is interesting to examine the time variations of these two components. As marked for January SSTs in Figure 3, the prominent ENSO winters of 1957-58, 1965-66, 1972-73, 1976-77, 1982-83 and 1991-92 are characterized by the amplification of both 1st and 2nd components in phase. The combined coefficients of the 1st and 2nd components in Figure 3 are weighted means by their respective percentage variances, as listed in Table 1. In cases of the moderate to weak ENSO winters, either the 1st or 2nd component is amplified, but not both of them in phase. The following summer of an ENSO winter is not necessarily associated with the ENSO type SST anomalies. When the 1st and 2nd principal components are reversed following the ENSO winter (Fig. 3), the southeastern Pacific is occupied by extensive negative areas. Such is the case for July 1964, 1973, and 1988 when negative SST anomalies developed in this area.

When we subject the long–term (1955-92) SST means of the 12 months of the year to the principal component analysis, we obtain pattern vectors and time variations of coefficients as shown in Figure 4 for the 1st and 2nd components. The variations of pattern vectors are concentrated in the tropical latitudes, and the time variations of both the 1st and 2nd components reflect the time scale of seasonal variations. Comparing the pattern vectors of 4 separate months in Figures 2 and 5, it is seen that basic patterns of 3 principal components seem to hold throughout the year, but are subject to the seasonal changes which are not negligible in terms of strength and local modification. The intra–annual seasonal variations presented in Figure 4 should be considered when the persistence of prevailing SST anomalies is to be projected. The pattern vectors of January and July, as shown in Figure 2, are modified between winter and summer to exhibit spring and fall patterns, as shown in Figure 5 for April and October.

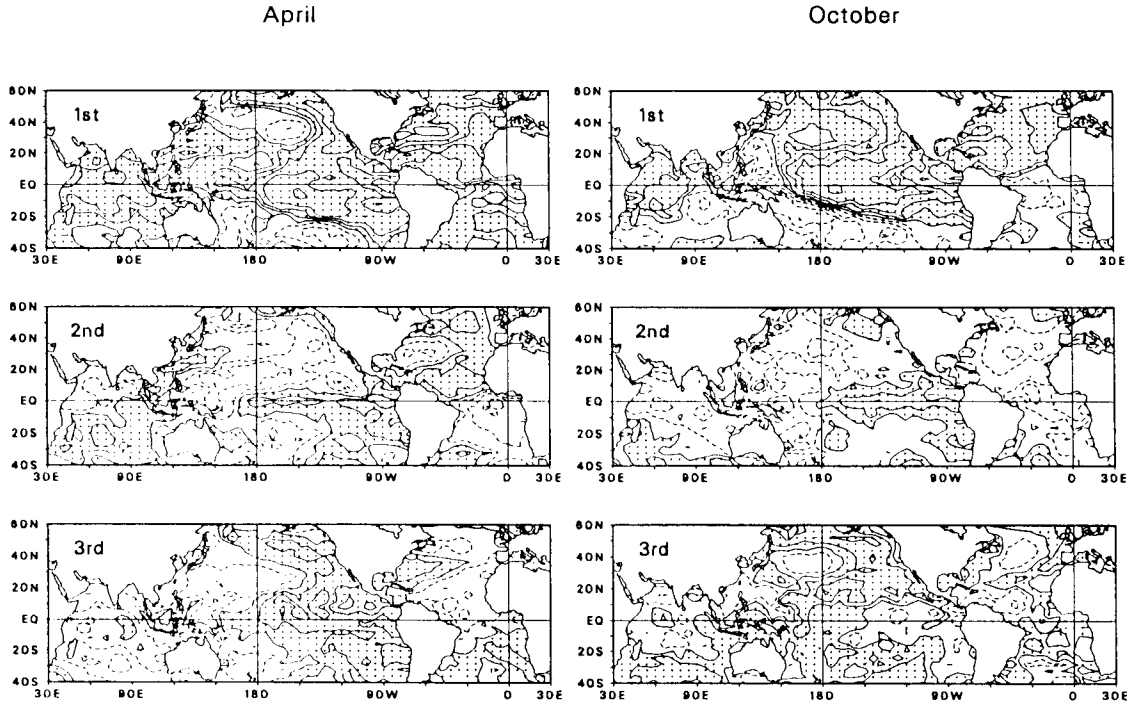


Fig. 5. Characteristic patterns for the first three principal components of April and October SSTs during the period of 1955-92. Positive areas are shaded. The contour interval is 0.2.

## 4. Principal components of the Northern Hemisphere circulation

Pattern vectors of the first three components of the Northern Hemisphere circulation in terms of January and July Z fields are shown in Figures 6, 7 and 8 respectively at the 700, 500 and 300 mb levels. A similarity in pattern is observed through the troposphere from 700 mb to 300 mb, and the 2nd component shows the best similarity at all three levels with "centers of action" in the same quadrants. These centers of action are stable and dominant, and consistent with the generally recognized winter flow patterns. As the first two components of winter Z fields determine the general pattern of the winter Northern Hemisphere flow, it is also noted in Table 1 that the contribution of percentage variance in the winter flow by the 2nd Z component is much greater than those by the 2nd components in SST and summer Z. The 3rd component, among the first three components, shows the more localized patterns, which is a generally observed character of higher components in the principal component analysis.

When the July patterns are compared to the January patterns in Figures 6-8, it is apparent that the patterns of all summer components are weakened at all levels, and the scale of dominant patterns becomes generally small. The distinguished patterns of the 2nd and 3rd components in winter become fragmented in summer with the sharpest constrast at 500 mb. However, components in summer show general consistency at different levels. The contrast between the summer and winter patterns merely reflects the difference between the dominant winter circulation and the significantly weakened summer circulation in the Northern Hemisphere.

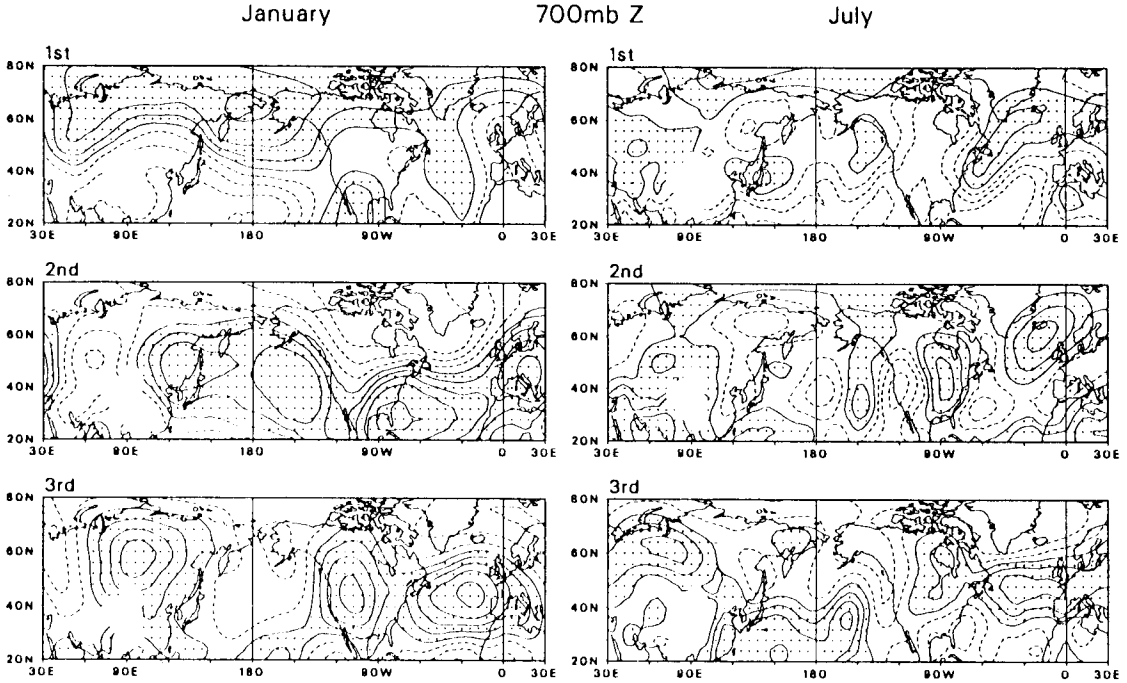


Fig. 6. Characteristic patterns of the first three principal components of 700 mb Z field in the Northern Hemisphere for January and July. The contour interval is 0.2 with real lines for zero and positive, and broken lines for negative.

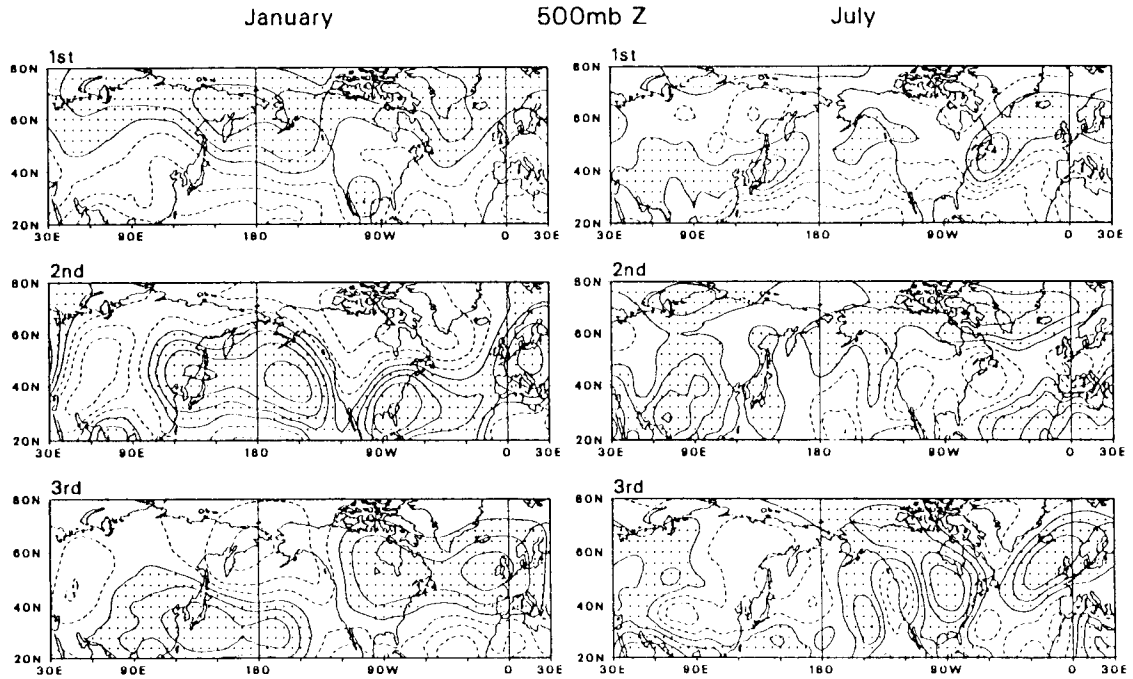


Fig. 7. As in Fig. 6, but for 500 mb.

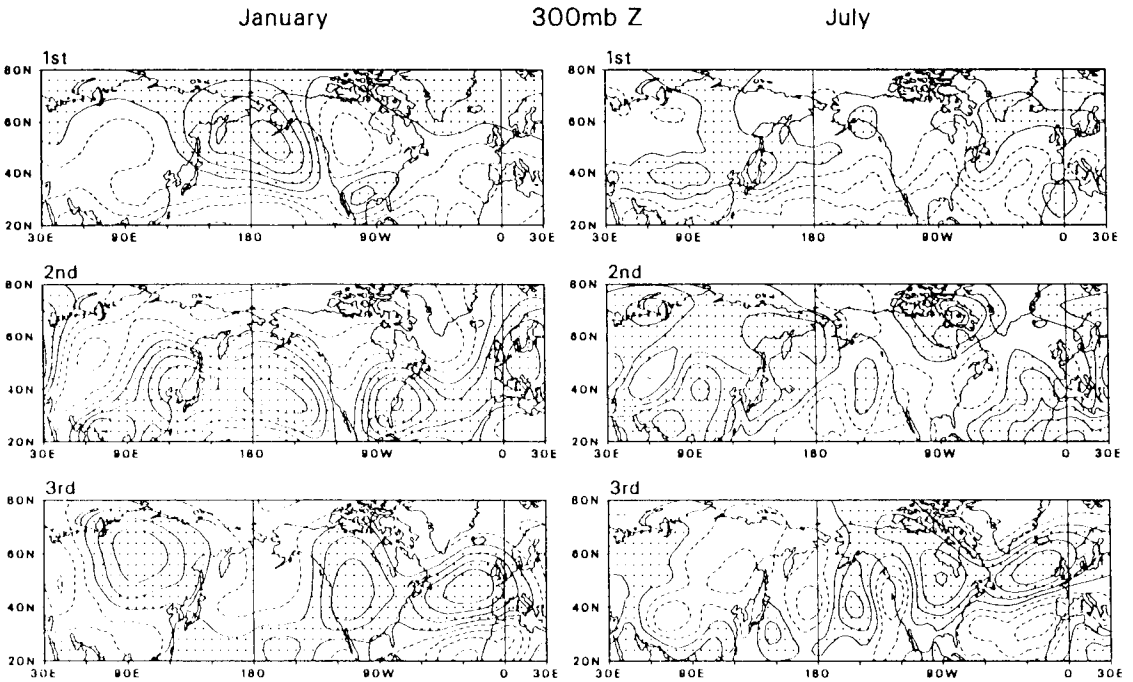


Fig. 8. As in Fig. 6, but for 300 mb.

Explicit association of physical processes with separate components of the circulation fields is beyond the scope of the principal component analysis. However, because of the lower bondary forcing of SSTs, it is useful to examine the correlations between components of SSTs and Z fields.

Table 2 lists the correlation coefficients between the first three components of SSTs in January, April, July and October, and those of monthly Z fields at 700, 500 and 300 mb during the period of 1955-92. The correlation coefficient | 0.35 | is significant at the 95% level, and | 0.44 | at the 99% level. In Table 2 it is evident that the 1st SST component is strongly correlated with the 1st Z component. The correlation is large at 300 mb and 500 mb throughout the year, particularly at 300 mb. However, at 700 mb it is limited to the winter season. In other words, the correlation of the 1st components of SSTs with the Z components is more significant in the upper troposphere than in the lower troposphere. The correlation of the 2nd and 3rd SST components with Z components is generally low. Although some sporadic correlations exist in the table, they do not indicate an organized pattern of correlation. According to the correlations in Table 2, only the 1st SST component shows a singificant, persistent correlation with the 1st Z component in the mid and upper troposphere.

Table 2. Correlation coefficients between principal components of monthly SSTs and principal components of monthly Z fields at 700, 500 and 300 mb during the period of 1955-92.

| SST(1st) | January | | | April | | | July | | | October | | |
|---|---|---|---|---|---|---|---|---|---|---|---|---|
| Z | Jan | Feb | Mar | Apr | May | Jun | Jul | Aug | Sep | Oct | Nov | Dec |
| 700 mb | | | | | | | | | | | | |
| (1st) | -.48 | -.63 | -.60 | -.53 | .25 | .44 | -.28 | -.34 | .22 | -.06 | -.29 | .51 |
| (2nd) | .46 | .03 | -.19 | -.06 | -.45 | .24 | -.27 | .02 | .43 | .62 | -.19 | .09 |
| (3rd) | -.18 | .11 | -.20 | -.35 | .40 | -.24 | -.04 | .50 | .13 | .43 | .31 | .05 |
| 500 mb | | | | | | | | | | | | |
| (1st) | -.36 | -.55 | .48 | -.49 | .43 | -.61 | -.45 | -.45 | .24 | -.26 | -.12 | -.51 |
| (2nd) | -.43 | -.04 | -.18 | -.23 | -.01 | .24 | -.08 | .15 | -.13 | .08 | -.04 | .12 |
| (3rd) | .09 | -.05 | -.23 | -.18 | -.24 | -.17 | .13 | .13 | .06 | -.47 | .56 | .12 |
| 300 mb | | | | | | | | | | | | |
| (1st) | .56 | .71 | .75 | .65 | .75 | -.84 | .64 | .60 | .61 | .34 | .25 | .49 |
| (2nd) | .22 | -.15 | .16 | .18 | .17 | .14 | -.17 | -.05 | .11 | .13 | -.23 | .04 |
| (3rd) | -.21 | -.16 | .12 | -.18 | .25 | -.01 | .05 | -.19 | .09 | .36 | .42 | -.05 |

| SST(2nd) | January | | | April | | | July | | | October | | |
|---|---|---|---|---|---|---|---|---|---|---|---|---|
| Z | Jan | Feb | Mar | Apr | May | Jun | Jul | Aug | Sep | Oct | Nov | Dec |
| 700 mb | | | | | | | | | | | | |
| (1st) | -.27 | -.46 | -.19 | .17 | .02 | .03 | -.20 | -.06 | .02 | -.06 | -.16 | .02 |
| (2nd) | .20 | -.05 | -.08 | .37 | .17 | -.11 | .20 | .06 | -.30 | .20 | -.29 | .18 |
| (3rd) | .01 | -.29 | .08 | .15 | -.09 | -.16 | -.02 | -.01 | .17 | .08 | .05 | -.23 |
| 500 mb | | | | | | | | | | | | |
| (1st) | -.06 | -.22 | .04 | -.01 | .01 | -.02 | -.33 | -.34 | .19 | .35 | .21 | .00 |
| (2nd) | -.11 | -.10 | -.07 | .34 | -.07 | .06 | .04 | .09 | .42 | -.04 | -.21 | -.33 |
| (3rd) | .45 | .49 | .00 | -.33 | -.15 | -.03 | -.27 | .17 | -.10 | -.18 | -.10 | .07 |
| 300 mb | | | | | | | | | | | | |
| (1st) | .09 | .23 | .12 | -.15 | -.22 | .21 | .25 | .39 | .26 | -.19 | -.11 | .06 |
| (2nd) | -.01 | .11 | .13 | -.25 | .04 | .12 | -.13 | -.14 | -.03 | .02 | -.09 | -.34 |
| (3rd) | .05 | .44 | .11 | -.26 | .25 | .14 | .43 | -.04 | .43 | -.11 | -.01 | .04 |

| SST(3rd) | January | | | April | | | July | | | October | | |
|---|---|---|---|---|---|---|---|---|---|---|---|---|
| Z | Jan | Feb | Mar | Apr | May | Jun | Jul | Aug | Sep | Oct | Nov | Dec |
| 700 mb | | | | | | | | | | | | |
| (1st) | -.32 | .11 | .03 | .24 | -.32 | -.03 | -.03 | -.00 | -.20 | .15 | -.19 | .23 |
| (2nd) | -.61 | .02 | -.01 | -.01 | -.29 | .40 | .43 | .08 | -.04 | -.21 | -.20 | .00 |
| (3rd) | -.01 | .04 | .30 | -.35 | .11 | .18 | -.18 | -.34 | -.26 | -.13 | .01 | -.18 |
| 500 mb | | | | | | | | | | | | |
| (1st) | -.26 | .04 | .11 | .28 | -.42 | .14 | -.16 | -.18 | .17 | .08 | -.02 | -.19 |
| (2nd) | .64 | .04 | -.04 | -.05 | .05 | -.22 | .01 | -.25 | .12 | -.16 | -.23 | -.15 |
| (3rd) | -.03 | -.17 | .18 | -.08 | .25 | -.13 | -.27 | -.17 | .09 | -.03 | .19 | .04 |
| 300 mb | | | | | | | | | | | | |
| (1st) | -.04 | -.22 | -.08 | -.17 | -.24 | .04 | -.09 | -.22 | -.29 | -.05 | -.01 | .12 |
| (2nd) | -.66 | -.04 | -.04 | .12 | .03 | -.05 | .07 | -.28 | -.03 | .11 | .17 | -.23 |
| (3rd) | -.01 | -.20 | .01 | .01 | -.18 | -.07 | -.04 | -.01 | .17 | .08 | .15 | .17 |

As the 1st and 2nd SST components seem to determine the occurrence of ENSO events (Fig. 3), it will be interesting to examine if the principal components of the upper–air circulation show a specific ENSO mode as in SSTs. Figure 9 illustrates the composite 700 mb and 500 mb flow pattern and anomaly fields for the prominent ENSO January months of 1958, 1966, 1973, 1977, 1983 and 1992. The 700 mb anomaly field resembles the pattern vectors of the 2nd principal component of the January 700 mb field (Fig. 6), and the 500 mb anomaly field shows a similarity to the pattern vectors of the 3rd principal component of the January 500 mb field. It is noted, however, that the inter–annual variations of such principal components are not clearly associated with winter ENSO occurrence. The situation is thus different from that of the time variations of SST components in association with ENSO occurrence (Fig. 3). Although SSTs show a clear large–scale mode of boundary forcing in ENSO winters, the responding upper–air circulation does not show such clear ENSO components. The anomalous circulation patterns, as often identified in ENSO winters, seem to be modifications of the basic field of circulation rather than dominant specific large–scale patterns.

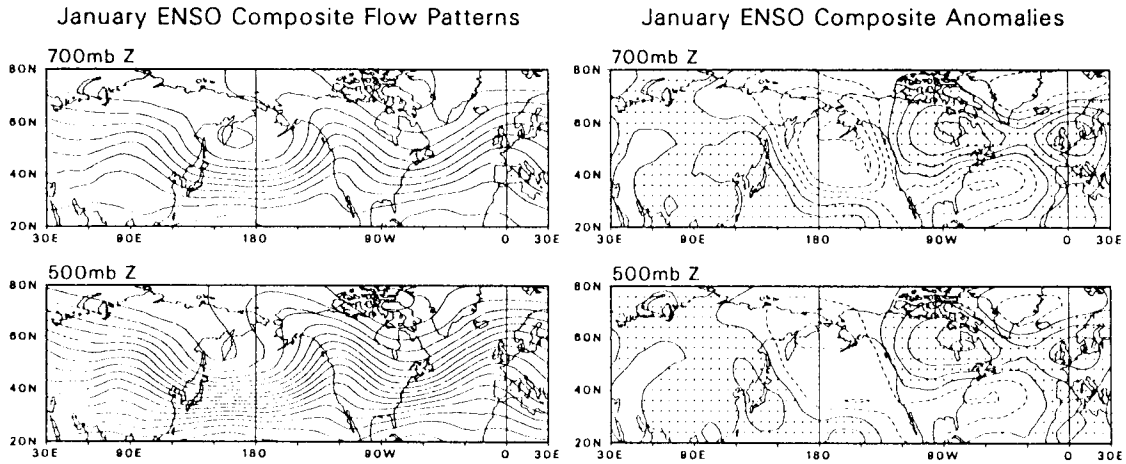


Fig. 9. 700 mb and 500 mb January flow patterns and anomalies for composites of prominent January ENSO cases.

## 5. Cross–correlation patterns

In a lag–correlation analysis, Kawamura (1986) demonstrated that time coefficients of the first component of the monthly mean North Pacific SST tends to lead the 500 mb Z in the extratropical latitudes. The lead time is up to 12 months or more, depending on the month of SST. Park and Kung (1988) showed that the SST anomalies for preceding seasons in the North Pacific are closely related to the first component of surface temperatures in North America in the following summer. The latter determines the summer temperature in the midwestern and mid–Atlantic United States. It is possible that the principal components of SST fields may be useful in the long– (seasonal–) range empirical forecast.

Figures 10, 11 and 12, respectively, illustrate the cross–correlation patterns between the 1st, 2nd and 3rd principal components of January SSTs and the January, April and July anomaly fields of 500 mb and 300 mb Z. All three SST components are well correlated to the 500 mb and 300 mb Z field of the same month, January. The contour spacing is 0.2, and the correlation in the figure is significant at 90, 95, 99 and 99.5% with the coefficients of | .0.28 |, | 0.33 |, | 0.42 | and | 0.45 |. In April, with a lead time of 3 months, all three SST components show similarities with January flow patterns. Some variations from the January patterns, particularly

the strengthening of the 2nd component correlation in April is noted. The correlations become weaker and more fragmented in July, apparently reflecting the weaker and more fragmented circulation patterns of the summer. However, the centers of action as recognized in earlier months in Pacific, Atlantic, North America and Eurasia are still traceable.

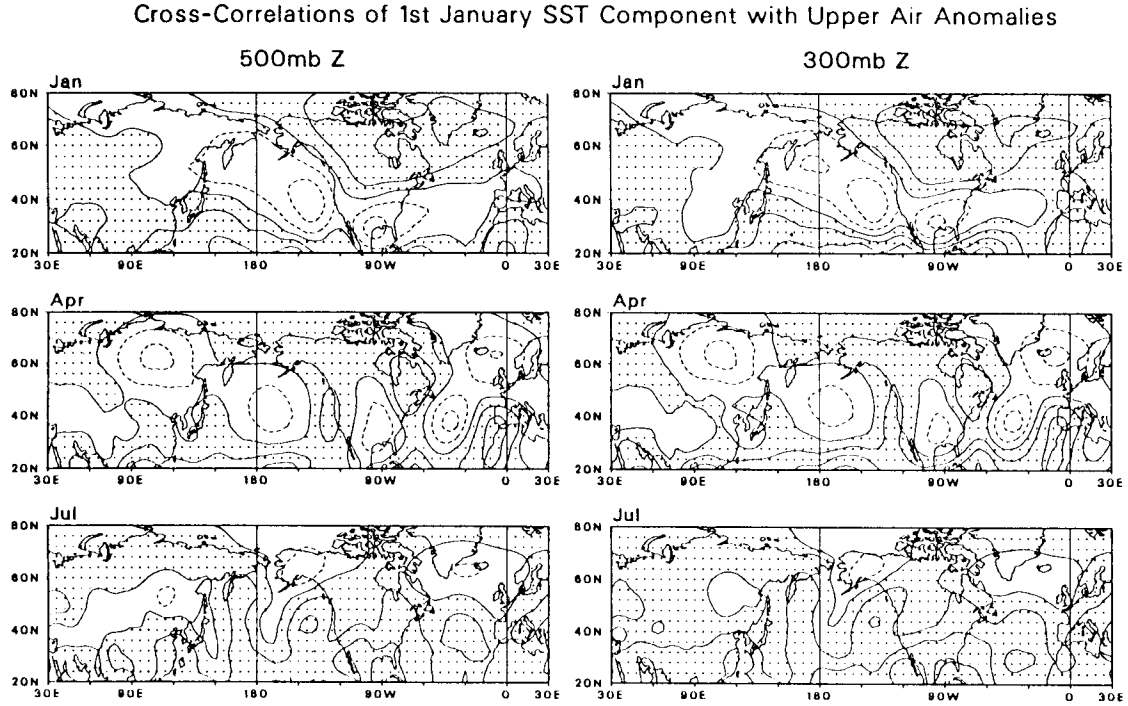


Fig. 10. Cross-correlation patterns of coefficients of the first January SST component and 500 mb and 300 mb Z fields in January, April and July. The contour interval is 0.2 with real lines for zero and positive, and broken lines for negative.

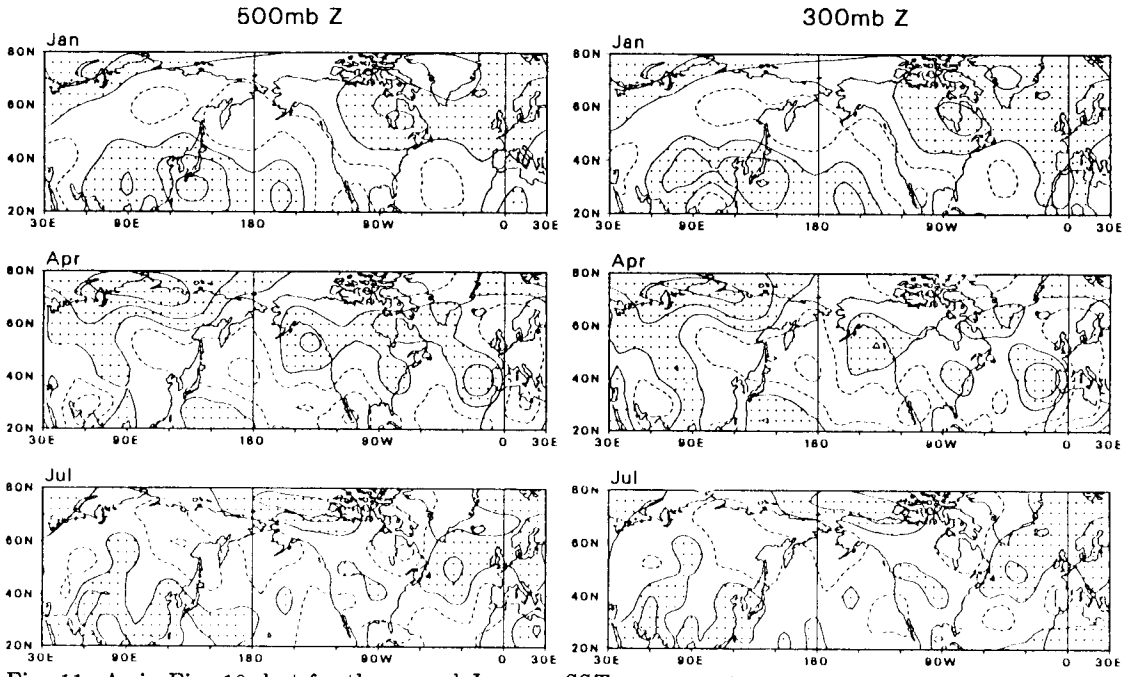


Fig. 11. As in Fig. 10, but for the second January SST component.

Comparing cross-correlations of January SST components with 500 mb and 300 mb flow patterns in Figures 10-12, it is noted that the characteristic correlation patterns, as observed with 500 mb fields, are identified in 300 mb Z fields in terms of both spatial distribution and strength of correlation coefficients. This suggests that the response of tropospheric circulation to SST anomaly fields is consistent in the mid and upper troposphere.

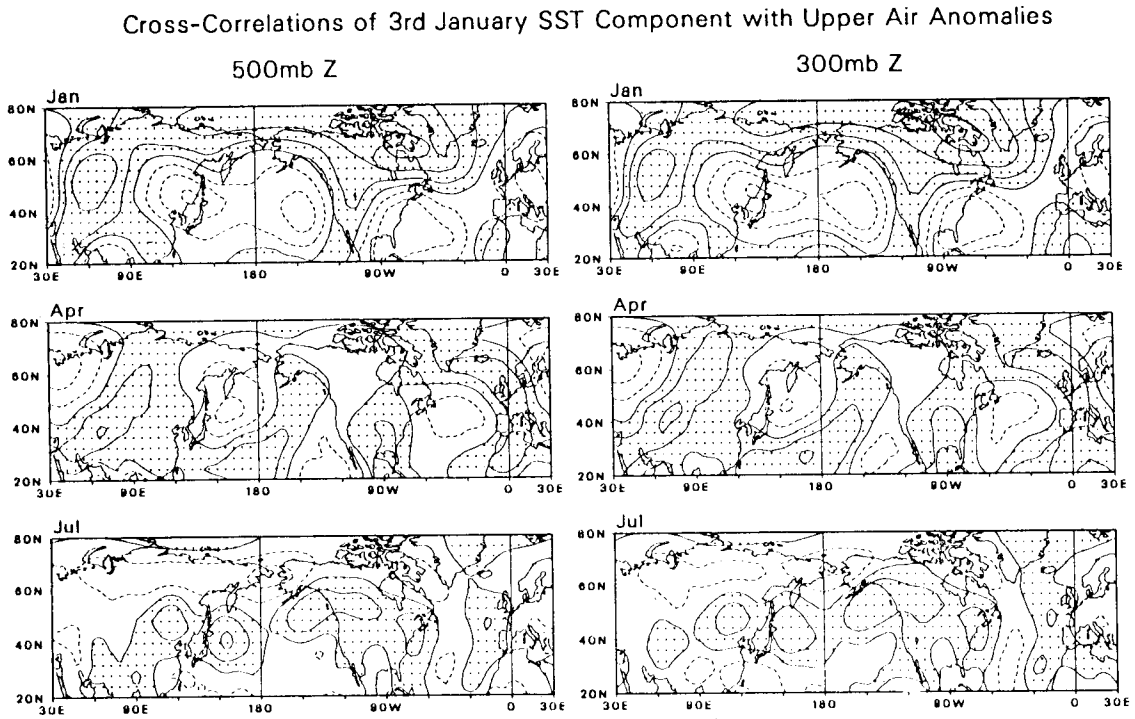


Fig. 12. As in Fig. 10, but for the third January SST component.

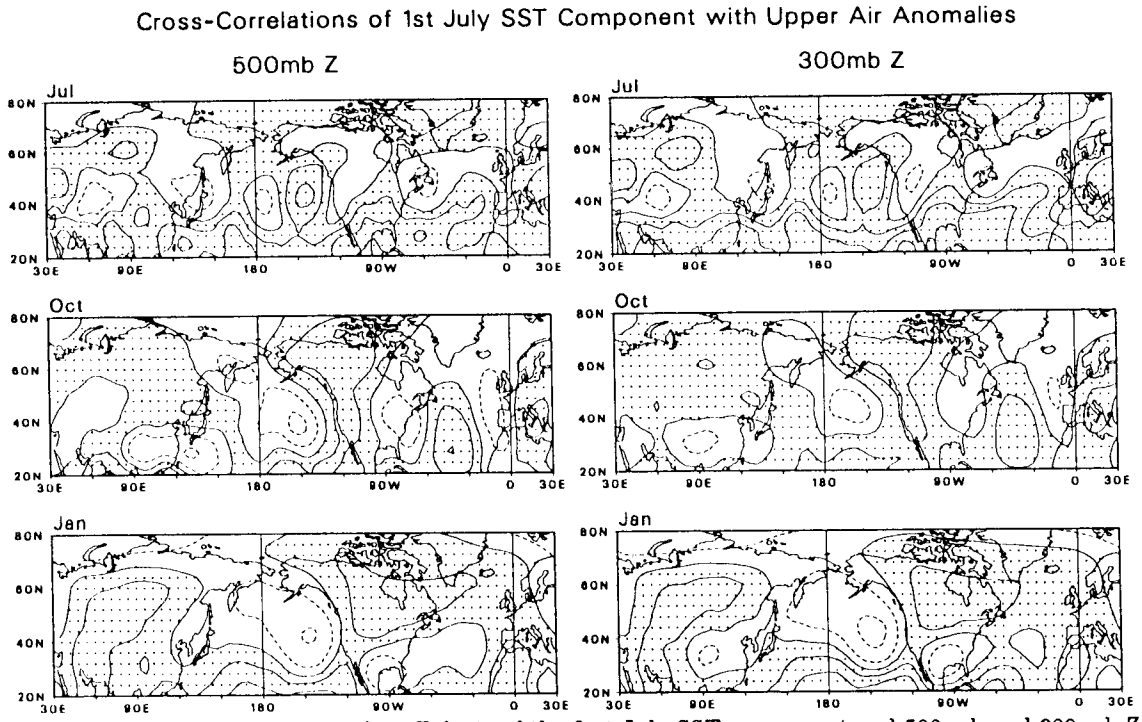


Fig. 13. Cross-correlation patterns of coefficients of the first July SST component and 500 mb and 300 mb Z fields in July, October and January.

The cross–correlation patterns of the 1st, 2nd and 3rd principal components of July SSTs with the July, October and January 500 mb and 300 mb Z fields are illustrated in Figures 13, 14 and 15. The cross–correlation patterns observed in July carry through October and January.

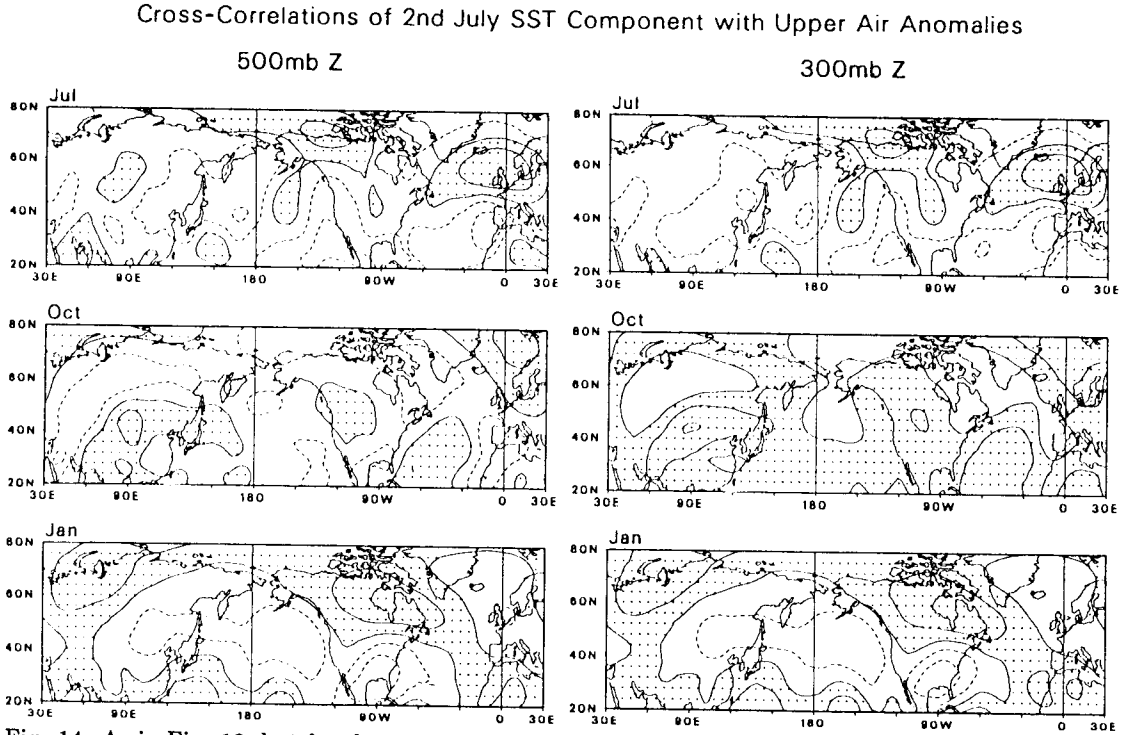


Fig. 14. As in Fig. 13, but for the second July SST component.

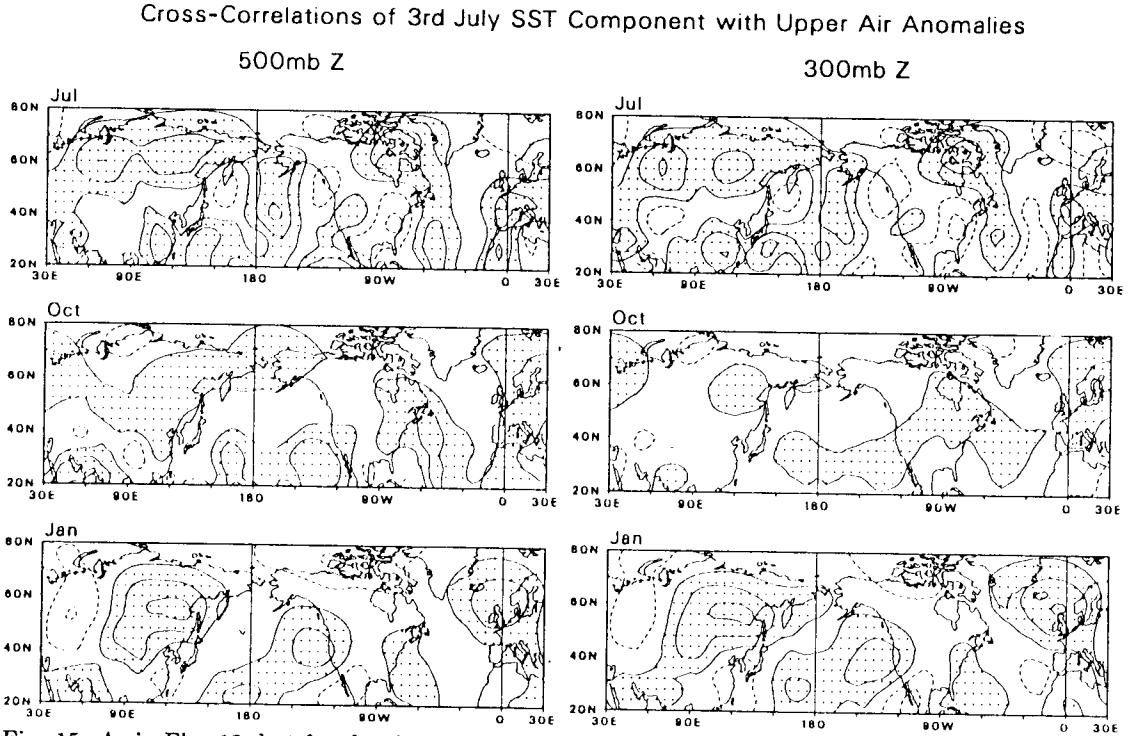


Fig. 15. As in Fig. 13, but for the third July SST component.

The patterns observed in 500 mb are also clearly observed in 300 mb. One clear distinction from the January SST cross–correlation is the strong correlation pattern of July SSTs with January 500 mb and 300 mb Z fields with a lead time of at least 6 months. It is also noteworthy that the cross–correlation with the January Z fields is stronger than with the October Z fields. Those observations reflect strong winter circulation patterns, and also indicate a useful seasonal–range predictability of winter upper–air circulation patterns with the anomaly fields of summer SSTs.

## 6. Concluding remarks

As stated in the introduction, the purpose of this paper is to identify prevailing modes of variations in SSTs and the tropospheric circulation. The results obtained in this study offer useful information in further diagnosis of the SST and circulation fields, and also the utilities of the SST anomaly field in seasonal–range forecasting of the tropospheric circulation. The principal component analysis of monthly mean fields of the global SSTs and the Northern Hemisphere tropospheric circulation for the 38–year period as presented in this study seems to yield the following specific information:

1. A change in the source of SST data results in a large systematic bias in a long–term SST dataset. However, the bias may be effectively corrected if an appropriate principal component is identified and eliminated from the dataset.
2. Periods of strong ENSO correspond to both the 1st and 2nd SST components being in phase.
3. The first few principal components of monthly SST and Z fields are sufficient to describe the SST and tropospheric circulation patterns.
4. Basic patterns of the first three principal components of SSTs remain similar throughout the year, but are subject to seasonal changes, which are not negligible.
5. The first SST component is strongly correlated with the first component of tropospheric Z field.
6. Cross–correlations of SST components with the tropospheric circulation suggest a useful predictability of the tropospheric circulation in reference to SST anomalies. The lead time observed in this study is up to 6 months for the winter circulation in reference to summer SSTs.

## Acknowledgements

This research was supported by the National Aeronautics and Space Administration/Goddard Space Flight Center (NAS5-30957). The authors are indebted to Ms. D. C. Marsico of the National Meteorological Center for providing the NMC sea surface temperature analyses, and to Ms. L. A. Farmer for providing technical support.

## REFERENCES

Barnett, T. P., 1978. Estimating variability of surface air temperature in the Northern Hemisphere. *Mon. Wea. Rev.*, **106**, 1353-1367.

Heddinghaus, T. K., and E. C. Kung, 1980. An analysis of climatological patterns of the Northern Hemispheric circulation. *Mon. Wea. Rev.* **108**, 1-17.

Kawamura, R., 1984. Relation between atmospheric circulation and dominant sea surface temperature anomaly patterns in the North Pacific during the northern winter. *J. Meteor. Soc. Japan*, **62**, 910-916.

Kawamura, R., 1986. Seasonal dependency of atmosphere–ocean interaction over the North Pacific. *J. Meteor. Soc. Japan*, **64**, 363-371.

Kidson, J. W., 1975a. Eigenvector analysis of monthly mean surface data. *Mon. Wea. Rev.*, **103**, 177-186.

Kidson, J. W., 1975b. Tropical eigenvector analysis and the Southern Oscillation. *Mon. Wea. Rev.*, **103**, 187-196.

Kutzbach, J. E., 1967. Empirical eigenvectors of sea–level pressure, surface temperature and precipitation complexes over North America. *J. Appl. Meteor.*, **6**, 791-802.

Kutzbach, J. E., 1970. Large–scale features of monthly mean Northern Hemisphere anomaly maps of sea–level pressure. *Mon. Wea. Rev.*, **98**, 708-716.

Overland, J. E., and R. W. Preisendorfer, 1982. A significant test for principal components applied to cyclone climatology. *Mon. Wea. Rev.*, **110**, 1-4.

Park, C.-K., and E. C. Kung, 1988. Principal components of the North American summer temperature field and antecedent oceanic and atmospheric conditions. *J. Meteor. Soc. Japan*, **66**, 667-690.

Reynolds, R. W., 1988. A real–time global sea surface temperature analysis. *J. Climate*, **1**, 75-86.

Slutz, R. J., S. J. Lubker, J. D. Hiscox, S. D. Woodruff, R. L. Jenne, D. H. Joseph, P. M. Steurer and J. D. Elms, 1985. COADS, Comprehensive Ocean–Atmosphere Data Set. Release 1, 262 pp. [Available from NOAA Climate Research Program, Environmental Research Laboratories, Boulder, CO 80303.]

Trenberth, K. E. and D. A. Paolino, 1981. Characteristic patterns of variability of sea level pressure in the Northern Hemisphere. *Mon. Wea. Rev.*, **109**, 1169-1189.

Walsh, J. E. and M. B. Richman, 1981. Seasonality in the associations between surface temperatures over the United States and the North Pacific Ocean. *Mon. Wea. Rev.*, **109**, 767-783.

Weare, B. C., 1977. Empirical orthogonal analysis of Atlantic Ocean surface temperature. *Quart. J. Roy. Meteor. Soc.*, **103**, 467-478.

Weare, B. C., A. R. Navato and R. E. Newell, 1976. Empirical orthogonal analysis of Pacific sea surface temperature. *J. Phys. Oceanogr.*, **6**, 671-678.